AIAA JOURNAL
Vol. 30, No. 5, May 1992

Patterns of Vortex Shedding from an Oscillating Circular Cylinder

Keun-Shik Chang* and Jong-Youb Sa†
Korea Advanced Institute of Science and Technology, Taejon, Republic of Korea

Vortex shedding from an oscillating circular cylinder was numerically investigated at $Re = 100$ using the Navier–Stokes equations and the new far-boundary stream-function condition. The detailed shedding patterns are delineated by means of the streakline plotting and the lift-coefficient curves. A parameter map is presented that distinguishes synchronized from asynchronous shedding and double-vortex from single-vortex shedding. The computational result is in good qualitative agreement with earlier experimental results.

Introduction

WHEN vortices are shed into the wake of a cylindrical body, they generally cause a periodic lift force on the body at the frequency of shedding and a drag force having twice that frequency. The interactive vibration of structures associated with these aerodynamic forces has been investigated by many researchers such as Savkar,[1] King,[2] and Sarpkaya.[3] The vortex shedding from the forcedly vibrating cylinder, which is the subject of the present paper, is a model simpler than the interactive-vibration model and yet can provide an understanding of complicated problems with many important applications.

The transverse cylinder vibration was studied by Koopman,[4] Griffin and Votaw,[5] and Griffin and Ramberg[6] whereas the streamwise oscillation was considered by Griffin and Ramberg,[7] Tatsuno,[8] and Tanida et al.[9] These experimental studies have revealed the following key features about vortex shedding from vibrating cylinders:

1) In some range of parameters, vortex shedding is synchronized with the cylinder vibration, which is known as the lock-in phenomenon.

2) The lift force increases greatly with the cylinder vibration, with its maximum response occurring near the center point of the lock-in frequency range.

3) The lateral spacing of the vortex street decreases with the amplitude of vibration. On the other hand, the longitudinal spacing varies inversely with the vibration frequency but is dependent on its amplitude.

For the streamwise vibration, two distinct patterns of vortex wake have been reported from the experiments. The first is a complex one in which two vortices are shed during each cycle of the vibration, whereas in the second a single vortex is shed during each cycle. When the oscillation amplitude is about $0.2d$ (d is the cylinder diameter), it is also known that the lateral spacing is reduced nearly to zero and the formation of the secondary vortex begins.

Numerical studies on vortex shedding have been primarily conducted for stationary cylinders. Oscillating cylinders, on the other hand, have been scarcely investigated by numerical methods: Hurlbut et al.[10] have calculated the aerodynamic force coefficients influenced by the streamwise vibration of the cylinder using the MAC method. Lecointe and Piquet[11] have computed vortex shedding from both the suddenly started and oscillating cylinders using the ADI method. Tamura et al.[12] have investigated vortex shedding for a transversely oscillating cylinder using the MAC method. Physical insight into the vortex-shedding patterns by means of a new accurate mathematical formulation and by streakline plotting is the goal of the present paper. A parameter map that shows the regions of synchronized shedding and double-vortex shedding was obtained in the present research.

Governing Equations and Boundary Conditions

In the present problem, a viscous incompressible fluid is assumed. A circular cylinder of radius a is placed transversely in a flow of uniform velocity U_∞. The Navier–Stokes equations are first written in terms of the vorticity and stream function in the cylindrical polar coordinates (r, θ). Coordinate transformation $r = e^{\pi\xi}$ (with normalization $\theta = \pi\eta$) allows grid refining toward the cylinder. The governing equations are then

$$\frac{\partial \zeta}{\partial t} + \frac{1}{(\pi r)^2}\left[\frac{\partial}{\partial \xi}\left(\zeta \frac{\partial \psi}{\partial \eta}\right)\right] - \frac{\partial}{\partial \eta}\left[\left(\zeta \frac{\partial \psi}{\partial \xi}\right)\right] = \frac{2}{Re}\tilde{\nabla}^2 \zeta \tag{1}$$

$$\tilde{\nabla}^2 \psi = -\zeta \tag{2}$$

where

$$\tilde{\nabla}^2 \equiv \frac{1}{(\pi r)^2}\left(\frac{\partial^2}{\partial \xi^2} + \frac{\partial^2}{\partial \eta^2}\right)$$

$$Re = \frac{(2a)U_\infty}{\nu}$$

The solutions of ζ and ψ are advanced in time by numerically integrating Eqs. (1) and (2). Central differencing is used, in general, for the space derivatives and forward differencing for the time derivative. However, the numerical modeling of the contravariant velocities ψ_ξ and ψ_η in the convection terms of the conservative form in Eq. (1) is important. Fourth-order Hermitian relations are used for this purpose in order to retain the conservation property of the scheme used, as well as accuracy. Equation (1) is solved by the Euler-explicit finite-difference scheme, and Eq. (2) by a direct elliptic solver called the stabilized error vector propagation (SEVP) method. The details of these numerical methods can be found in the authors' previous work.[13,14]

The error vector propagation (EVP) method is a direct method applicable to any type of elliptic equations. However, EVP is unstable when the number of grid points is large. Madala[15] proposed a modification of this method called SEVP (representing stabilized EVP), which is stable for any number of grid points and retains most of the advantages of the earlier EVP. In the SEVP method, the integration region is divided into directional blocks, each of which is not large so that the

Received March 1, 1990; revision received July 2, 1990; accepted for publication Aug. 1, 1990.

*Professor, Department of Aerospace Engineering, Kusong-dong 373-1, Yusung-gu. Member AIAA.

†Currently Senior Researcher, Samsung Electron Devices Inc., Whasung-gun, Kyong-gi-do, Republic of Korea.

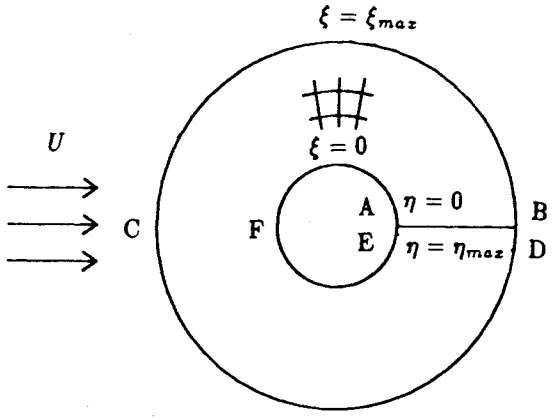

Fig. 1 Flow geometry.

EVP method remains stable. We have used the five-block SEVP method on the 51×50 grid systems, with $\Delta\xi = 0.02$, $\Delta\eta = 0.04$, and $\Delta t = 0.05$.

For the coordinate system moving with the cylinder (its origin is at the center of the cylinder), the following boundary conditions are used at the four boundaries ($\overline{AFE}$, $\overline{BCD}$, $\overline{AB}$, and $\overline{ED}$) shown in Fig. 1.

At $\xi = 0$ ($\overline{AFE}$),

$$\zeta_w = \tilde{\nabla}^2\psi|_w, \qquad \psi_w = 0$$

and at $\xi = \xi_{\max}$ ($\overline{BCD}$)

$$\zeta = 0 \quad \text{(at in flow boundary where } \frac{\partial\psi}{\partial\eta} < 0\text{)}$$

$$\frac{\partial\zeta}{\partial\xi} = 0 \quad \text{(at outflow boundary where } \frac{\partial\psi}{\partial\eta} > 0\text{)}$$

$$\psi = \psi_{\text{far}} \text{ (at entire boundary)}$$

where

$$\psi_{\text{far}} = Uy + \frac{1}{2\pi}\sum_{n=1}^{3}\frac{1}{n}G_n \sin(n\theta)\, r^{-n} + \mathcal{O}(r^{-4})$$

$$G_1 = \int\int \zeta y \, dS$$

$$G_2 = \int\int 2\zeta xy \, dS$$

$$G_3 = \int\int \zeta(3x^2y - y^3) \, dS$$

In the foregoing, ψ_{far} is the far-boundary stream function evaluated at the boundary of a finite computational domain and its derivation is explained in detail by Sa and Chang.[13] These conditions basically imply the no-slip condition on the body surface and the freestream condition, $U = U_\infty + u'$, at infinity (U_∞ is the freestream velocity and u' is the motion of the cylinder). On the cut boundaries, $\eta = 0$ ($\overline{AB}$) and $\eta = \eta_{\max}$ ($\overline{ED}$), continuous derivatives are enforced.

When a vortex is shed from the rear of the cylinder, periodic excursion of the forward stagnation point on the front part of the cylinder surface makes the wall stream function ψ_w oscillate. Jordan and Fromm[16] calculated the vortex shedding from a circular cylinder with an account of the oscillatory stagnation point, but it is known that its contribution is insignificant for low Reynolds numbers. In the present research conducted at the Reynolds number 100, the authors simply took the wall stream function as zero, following the practice of Borthwick,[17] to save computational time. It is noted that a comparison of the sample result of the present approach with that of Jordan and Fromm[16] (in terms of Strouhal number and drag coefficient) showed sufficiently good agreement; see Ref. 14.

The tangential gradient of pressure at the surface is

$$\frac{\partial p}{\partial\eta} = \frac{2}{Re}\frac{\partial\zeta}{\partial\xi} - \pi\frac{du'}{dt}\sin\theta$$

The surface pressure and skin friction, respectively, are obtained by

$$p_{j+1} = p_j + \frac{\Delta\eta}{Re}\left(\frac{\partial\zeta}{\partial\xi}\bigg|_j + \frac{\partial\zeta}{\partial\xi}\bigg|_{j+1}\right) - \pi\eta\frac{du'}{dt}\sin\theta_{j+\frac{1}{2}}$$

$$\tau_w = \frac{2}{Re}\zeta_w$$

The lift and drag coefficients are, finally,

$$C_L = \frac{\text{lift}}{\frac{1}{2}\rho U_\infty^2(2a)} = -\int p\sin\theta\, d\theta + \frac{2}{Re}\int \zeta_w\cos\theta\, d\theta \qquad (3)$$

$$C_D = \frac{\text{drag}}{\frac{1}{2}\rho U_\infty^2(2a)} = -\int p\cos\theta\, d\theta + \frac{2}{Re}\int \zeta_w\sin\theta\, d\theta \qquad (4)$$

Results and Discussion

The vortex shedding from the cylinder oscillating in the freestream direction is synchronized with the vibration of the cylinder, provided that it vibrates near twice the frequency of the natural shedding that would be obtained for a stationary cylinder, and also at the same time, provided that the vibration amplitude is beyond a certain threshold value that depends on the vibration frequency. This synchronization is sometimes called the "lock-in phenomenon." The lock-in range for the streamwise vibration of the circular cylinder has been investigated by Griffin and Ramberg,[7] Tatsuno,[8] and Tanida et al.[9] The present result for the lock-in range is shown in Fig. 2 and is compared with other experimental results. The detailed shedding pattern in the lock-in range was investigated here by streakline plotting. Two distinct patterns of vortex shedding are identified: A pair of vortices is shed in one cycle

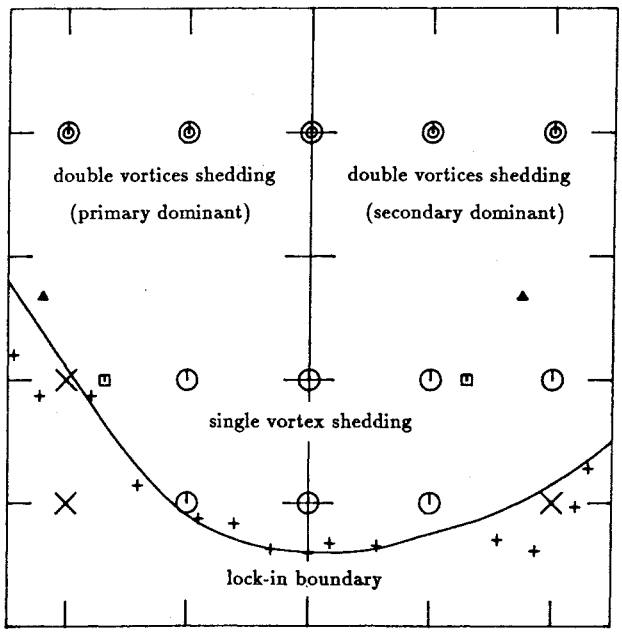

Fig. 2 Shedding map for the in-line vibration at $Re = 100$: ⓓ, double vortices shedding; ①, single vortex shedding; ×, asynchronous shedding. Lock-in boundary: +, Griffin and Ramberg[7] at $Re = 190$; ⊡, Tatsuno[8] at $Re = 100$; ▲, Tanida et al.[9] at $Re = 80$.

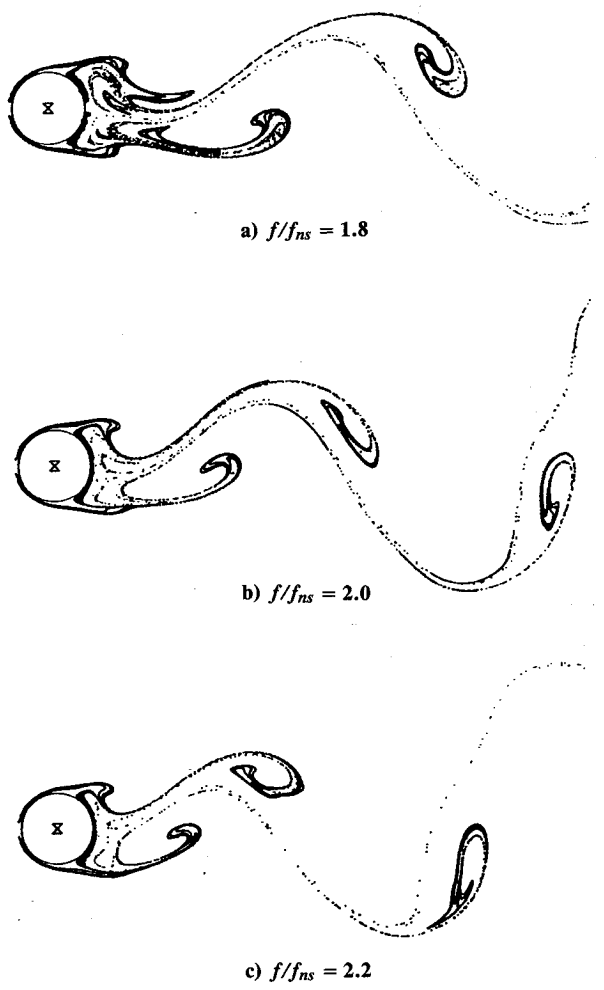

Fig. 3 Streaklines for the in-line vibration with amplitude ratio 0.1 at $Re = 100$.

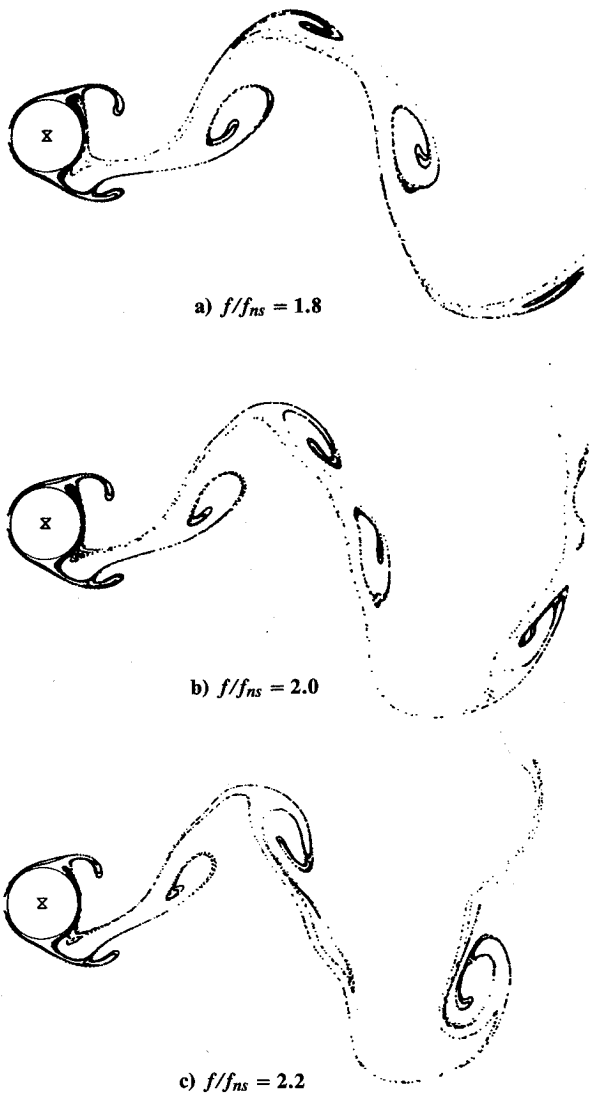

Fig. 4 Streaklines for the in-line vibration with amplitude ratio 0.4 at $Re = 100$.

of vibration in one pattern and an alternate vortex in the other pattern. When the amplitude ratio is relatively small but above the threshold of lock-in, the single vortex pattern is obtained. As the amplitude ratio is increased above about $0.2d$, the secondary vortex shedding is initiated by the cylinder motion and it is shed at the opposite side of the primary one to form the double-vortex-shedding pattern. This result is consistent with other experimental findings. Here, some new facts on interaction between the primary and secondary vortex are found, which will be explained in detail in Figs. 4–6.

The single-vortex pattern occurs over the entire lock-in frequency region as far as the amplitude ratio is lower than 0.2, but is above the threshold value, as shown in Fig. 2. The detailed shedding pattern is visualized in Fig. 3 in the near wake by the numerical streaklines. The longitudinal spacing of the vortex cores varies inversely with the vibration frequency and the lateral spacing is smaller than that of the stationary cylinder. The overall vortex street appears to have some similarity with the familiar single-vortex pattern seen from the stationary cylinder. However, careful observation reveals the existence of a vestige of the secondary vortex that did not develop into a separate vortex core. The fate of this incipient vortex can be different, depending on the vibration frequency. It is merged to the shear layer when the frequency ratio is near 2. At a frequency ratio higher than 2, it drifts downstream and is entrained into the primary vortex previously shed from the same side of the cylinder; at the frequency ratio lower than 2, it is entrained into the wake cavity to form a part of the core of the next primary vortex to come from the same side.

If the vibration amplitude increases above $0.2d$, the incipient secondary vortex grows into a tongue of the folded vortex sheet, which develops into the vortex core after elongation and rolling up. The tongue is observed at the amplitude ratio 0.2, but the plotting is presented in Fig. 4 for more distinguished vortices at the amplitude ratio 0.4. This incipient secondary vortex is generated at the same time as the primary one on the opposite side, both of which are shed simultaneously. Here, the interaction between the primary and secondary vortex follows because of the instability of the vortex street. The pattern of this interaction again depends on the vibration frequency, as shown in Fig. 4. When the frequency ratio is lower than 2, the primary vortex is dominant and the secondary one is subsequently merged by the shear layer downstream. As the frequency ratio increases above 2, the secondary vortex prevails over the primary one that is entrained and absorbed with time by the former. At the frequency ratio near 2, the primary and secondary vortex coexist with almost equal amplitude for some time in the near wake. The variance of the interaction pattern dependent on the vibration frequency can be explained in terms of the cylinder velocity. When the amplitude ratio is fixed, the velocity of the vibrating cylinder varies inversely with the frequency. The faster velocity of the cylinder or the higher frequency ratio will cause a stronger secondary vortex. Figure 5 shows the phase of vortex shedding and

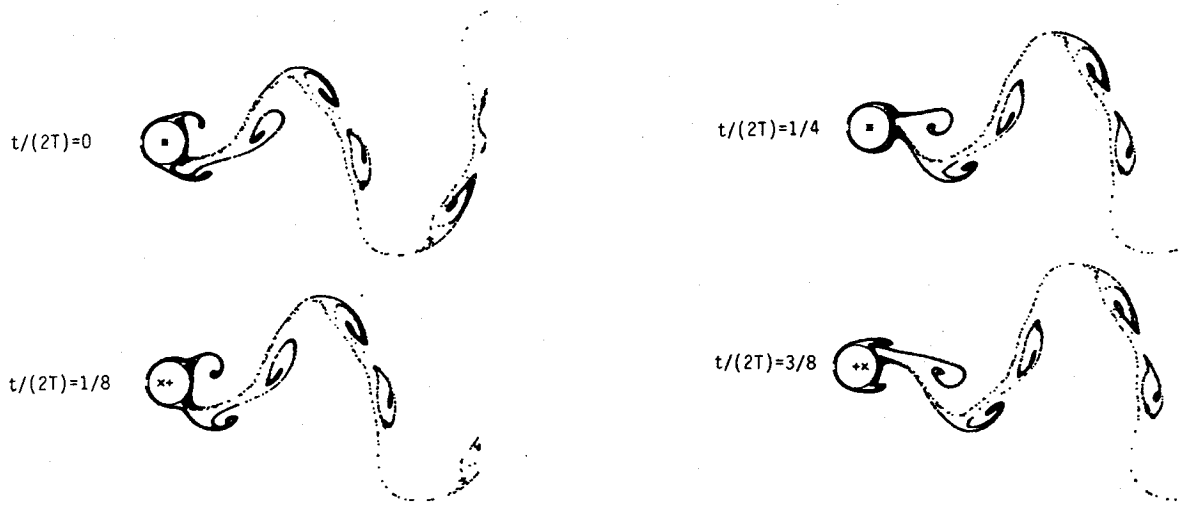

Fig. 5 Sequence of vortex shedding for the in-line vibration with amplitude ratio 0.4 and frequency ratio 2.0 at $Re = 100$.

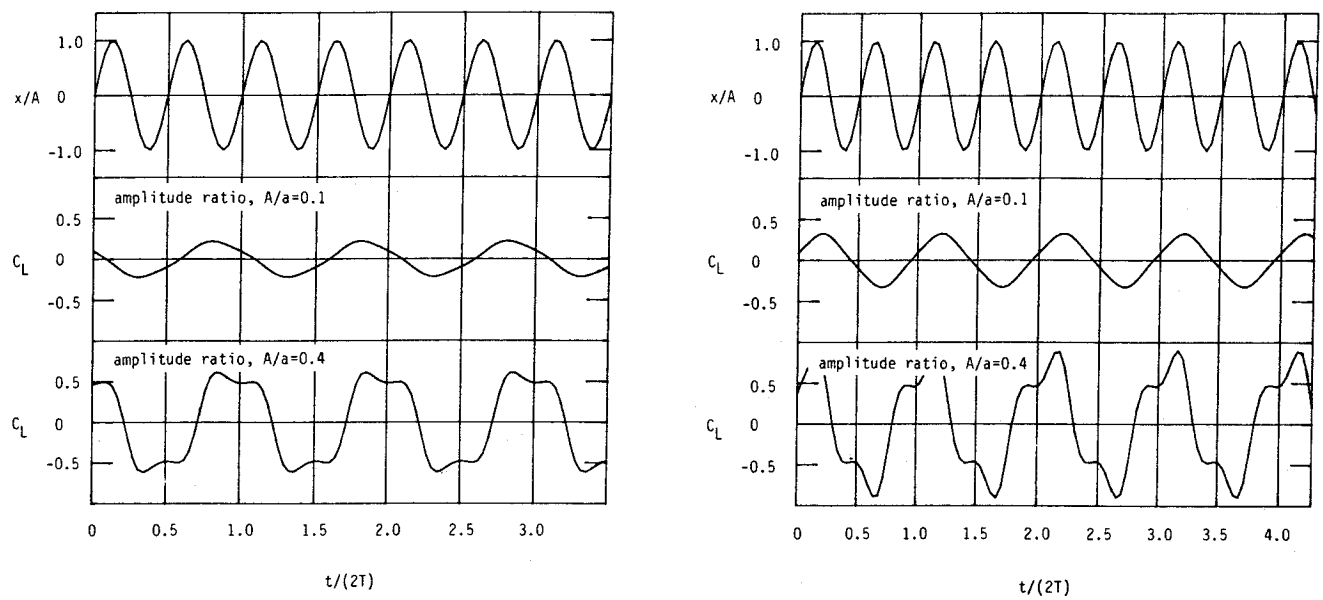

a) Frequency ratio, $f/f_{ns} = 1.8$

b) Frequency ratio, $f/f_{ns} = 2.2$

Fig. 6 Lift coefficient for the in-line vibration with amplitude ratio 0.1 and 0.4 at $Re = 100$.

a) Frequency ratio 1.6 and amplitude ratio 0.2

b) Frequency ratio 2.4 and amplitude ratio 0.1

Fig. 7 Shedding pattern in non-lock-in range.

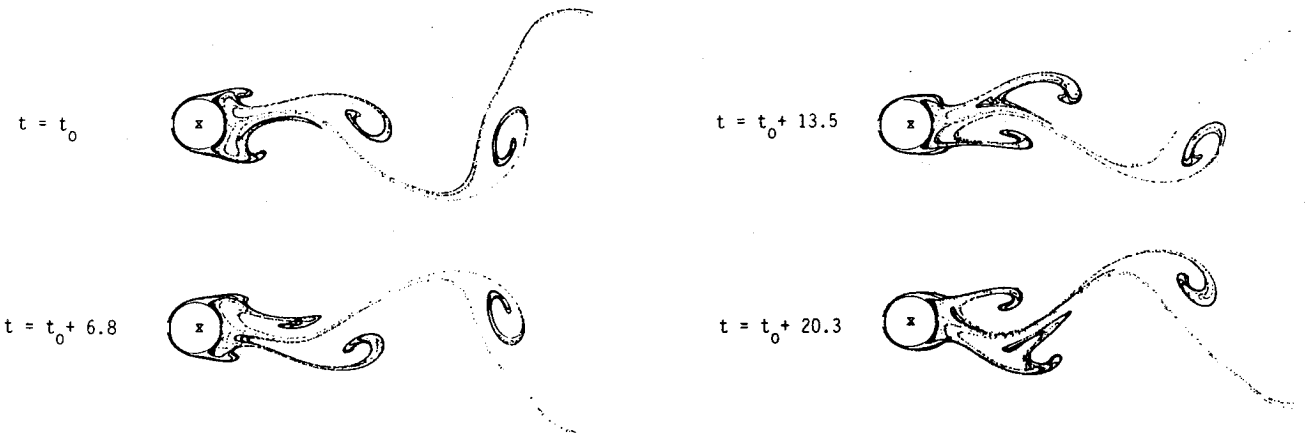

Fig. 8 Sequence of vortex shedding in non-lock-in range with frequency ratio 1.6 and amplitude ratio 0.2.

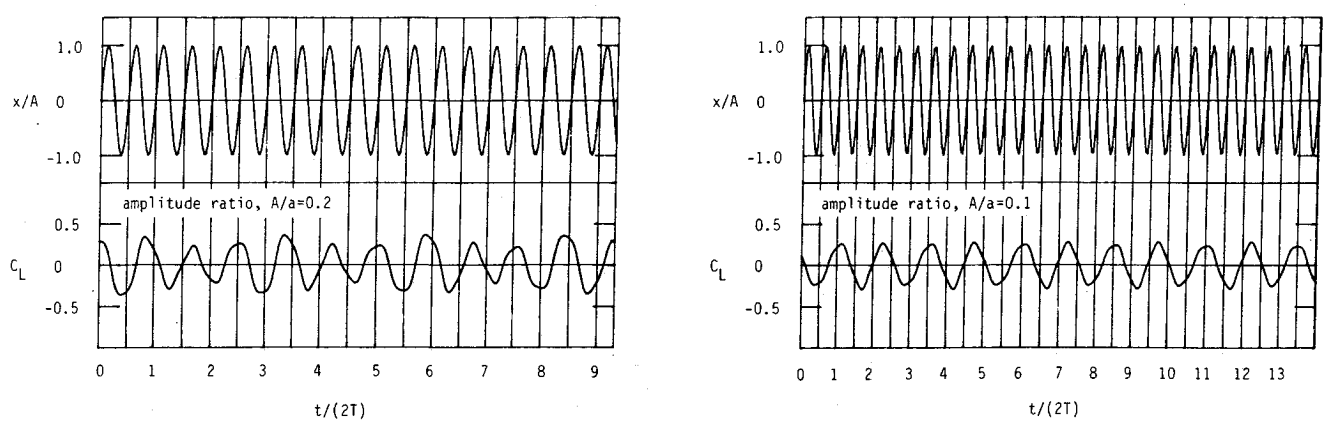

a) Frequency ratio, $f/f_{ns} = 1.6$

b) Frequency ratio, $f/f_{ns} = 2.4$

Fig. 9 Lift coefficient at non-lock-in range.

the interaction between the primary and the secondary vortices at the amplitude ratio 0.4 and frequency ratio 2.0.

The lift coefficient curves shown in Figs. 6a and 6b can be a useful tool in investigating the shedding patterns. The lift curve for the case of the single-vortex-shedding pattern has a single local peak during a cycle, whereas that from the double-vortex-shedding pattern shows double local peaks. The relative height of the double peak tells which vortex is stronger: when the primary vortex is dominant, the first peak rises above the second (see Fig. 6a for $A/a = 0.4$), and, conversely, the higher second peak implies that the primary vortex will be outgrown by the secondary one (see Fig. 6b for $A/a = 0.4$).

The vortex shedding in the non-lock-in range also can be nicely viewed by the numerical streaklines, as shown in Fig. 7. The shedding pattern is complicated in the near wake and cannot be characterized clearly, depending on the frequency or the amplitude of vibration. However, the Karman vortex street will eventually be formed downstream. The sequence of the nonperiodic shedding is shown in Fig. 8 for the amplitude ratio 0.2 and frequency ratio 1.6. The severe near-wake irregularity is noteworthy. The shedding frequency in this case is no longer strictly synchronized with the cylinder vibration and varies rather nonperiodically with time. The lift curves in Figs. 9a and 9b show no rigorous, but rather rough, periodicity, devoid of synchronization. The lift curve here is, however, not totally irregular either, since a similar shape is repeated every two or three cycles.

Conclusions

The vortex shedding from a cylinder vibrating forcedly in the stream direction is of two types: synchronized and asynchronous. Again, synchronized shedding can have either a single-vortex-shedding or double-vortex-shedding pattern. When the amplitude ratio is small but above the threshold value, a single vortex is alternately shed in a cycle. As the amplitude ratio is increased above 0.2, a pair of double vortices is shed in a cycle from the cylinder. This result agrees well with earlier experimental results.

In double-vortex shedding, the interaction between the primary and secondary vortex determines the fate of the vortex street to be followed. The primary vortex is dominant when the frequency ratio is lowered below 2, whereas the secondary vortex is more dominant when the frequency ratio is raised above 2.

The shedding patterns can be readily distinguished by the lift curve, which shows a single local peak for the single vortex shedding and two local peaks for double-vortex shedding. A comparison of the strength of the two peaks can suggest which will be more dominant: the primary or the secondary vortex.

References

[1]Savkar, S., "A Survey of Flow-Induced Vibrations of Cylinder Arrays in Cross Flow," *Journal of Fluids Engineering*, Vol. 99, No. 3, 1977, pp. 242–258.

[2]King, R., "A Review of Vortex Shedding Research and its Application," *Ocean Engineering*, Vol. 4, 1977, pp. 141–172.

[3]Sarpkaya, T., "Vortex Induced Oscillations, A Selective Review," *Journal of Applied Mechanics*, Vol. 46, No. 2, 1979, pp. 241–258.

[4]Koopmann, G. H., "The Vortex Wakes of Vibrating Cylinders at Low Reynolds Numbers," *Journal of Fluid Mechanics*, Vol. 28, Part 3, 1967, pp. 501–512.

[5]Griffin, O. M., and Votaw, C. W., "The Vortex Street in the Wake

of a Vibrating Cylinder," *Journal of Fluid Mechanics*, Vol. 51, Part 1, 1972, pp. 31–48.

[6]Griffin, O. M., and Ramberg, S. E.,"The Vortex-Street Wakes of Vibrating Cylinder," *Journal of Fluid Mechanics*, Vol. 66, Part 3, 1974, pp. 553–576.

[7]Griffin, O. M., and Ramberg, S. E., "Vortex Shedding from a Cylinder Vibrating in Line with an Incident Uniform Flow," *Journal of Fluid Mechanics*, Vol. 75, Part 2, 1976, pp. 257–271.

[8]Tatsuno, M., "Vortex Street Behind a Circular Cylinder Oscillating in the Stream Direction," *Bulletin of Research Institute of Applied Mechanics,* Kyushu University, Vol. 36, 1972, pp. 25–37 (in Japanese).

[9]Tanida, Y., Okajima, A., and Watanabe, Y., "Stability of a Circular Cylinder Oscillating in Uniform Flow or in a Wake," *Journal of Fluid Mechanics*, Vol. 61, Part 4, 1973, pp. 769–784.

[10]Hurlbut, S. E., Spaulding, M. L., and White, F. M., "Numerical Solution for Laminar Two Dimensional Flow about a Cylinder Oscillating in a Uniform Stream," *Journal of Fluid Engineering*, Vol. 104, 1982, pp. 214–222.

[11]Lecointe, Y., and Piquet, J., "On the Use of Several Compact Methods for the Study of Unsteady Incompressible Viscous Flow around a Circular Cylinder," *Computers & Fluids*, Vol. 12, No. 4, 1984, pp. 255–280.

[12]Tamura, T., Tsuboi, K. and Kuwahara, K., "Numerical Simulation of Unsteady Flow Patterns around a Vibrating Cylinder," AIAA Paper 88-0128, Reno, NV, Jan. 1988.

[13]Sa, J.-Y., and Chang, K.-S., "On Far-Field Stream Function Condition for Two Dimensional Incompressible Flows," *Journal of Computational Physics,* Vol. 91, No. 2, 1990, pp. 398–412.

[14]Sa, J.-Y., and Chang, K.-S., "Shedding Patterns of the Near-Wake Vortices behind a Circular Cylinder," *International Journal for Numerical Methods in Fluids,* Vol. 12, No. 5, 1991, pp. 463–464.

[15]Madala, R. V., "An Efficient Direct Solver for Separable and Non-Separable Elliptic Equations," *Monthly Weather Review*, Vol. 106, 1978, pp. 1735–1741.

[16]Jordan, S. K., and Fromm, J. E., "Oscillating Drag, Lift, and Torque on a Circular Cylinder in a Uniform Flow," *Physics of Fluids*, Vol. 15, No. 3, 1972, pp. 371–376.

[17]Borthwick, A., "Comparison Between Two Finite-Difference Schemes for Computing the Flow around a Cylinder," *International Journal for Numerical Methods in Fluids*, Vol. 6, No. 5, 1986, pp. 275–290.